Supplemental Figure 1

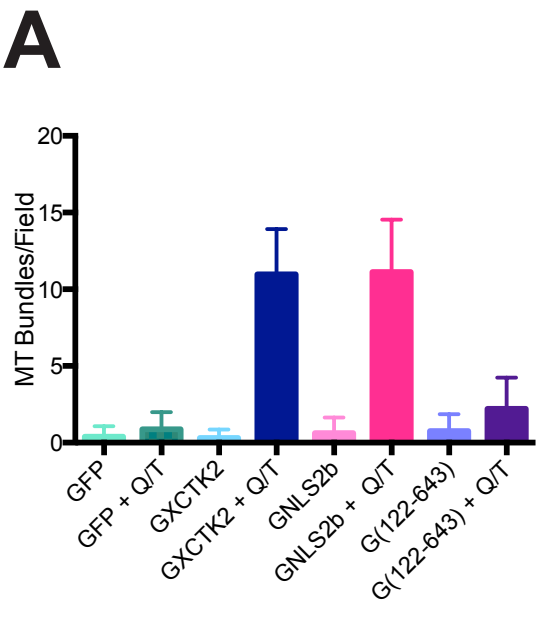

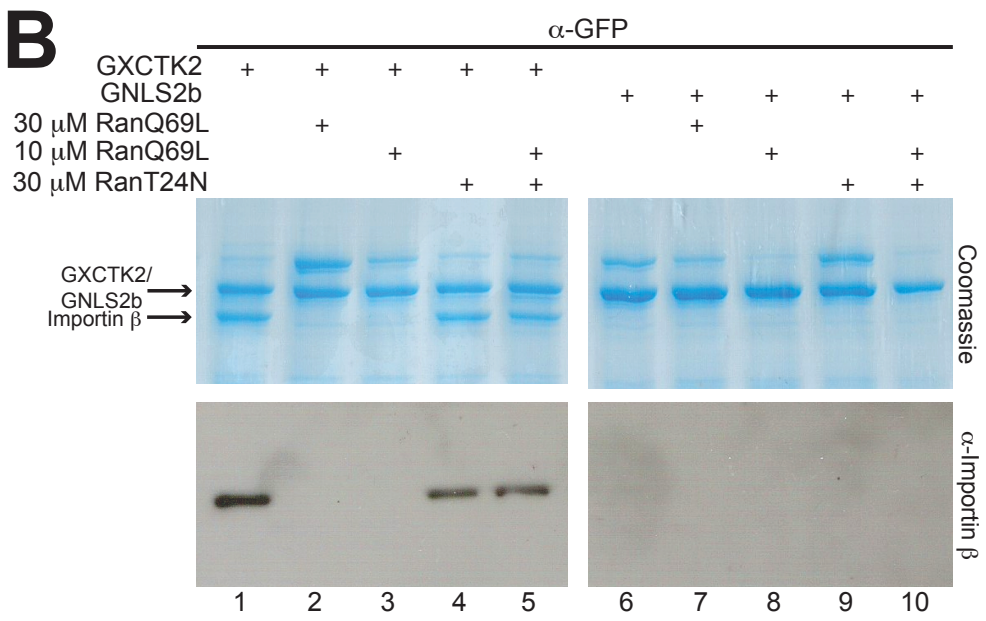

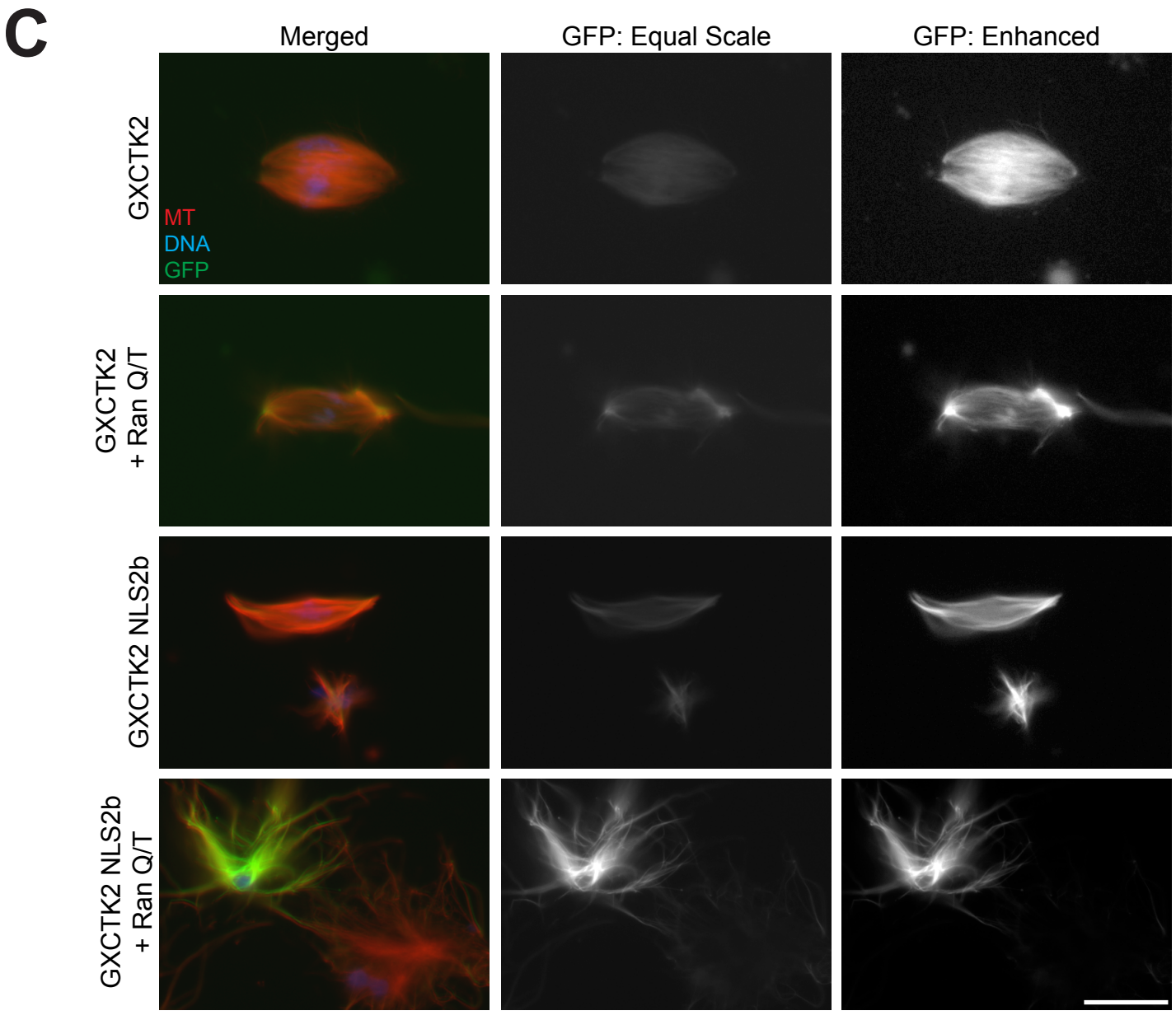

Supplemental Figure 2

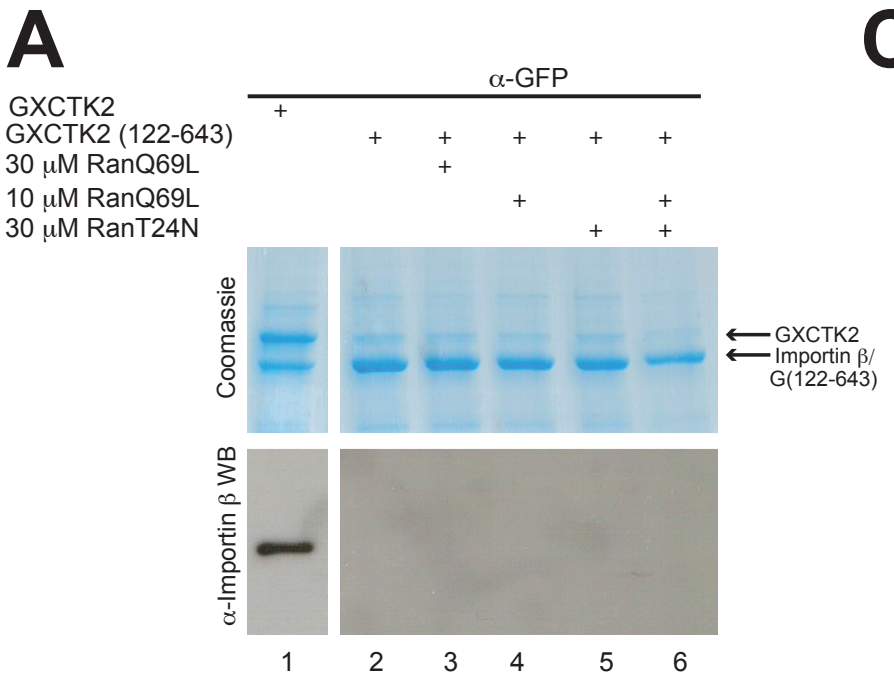

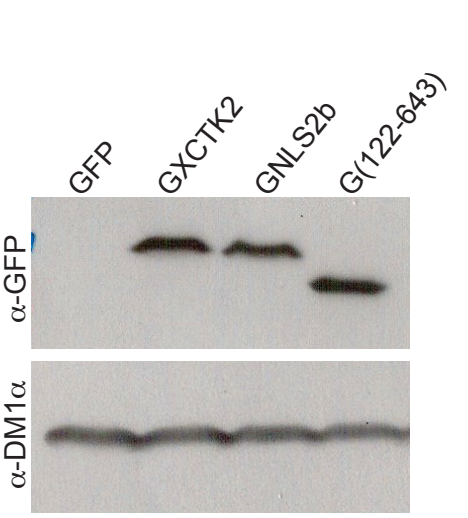

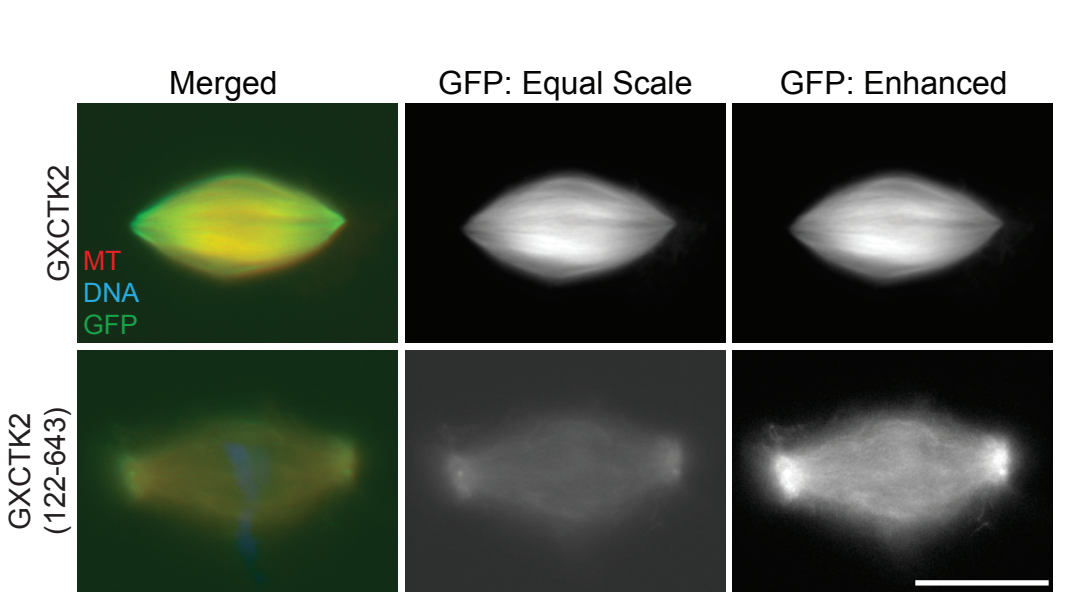

Supplemental Figure 3

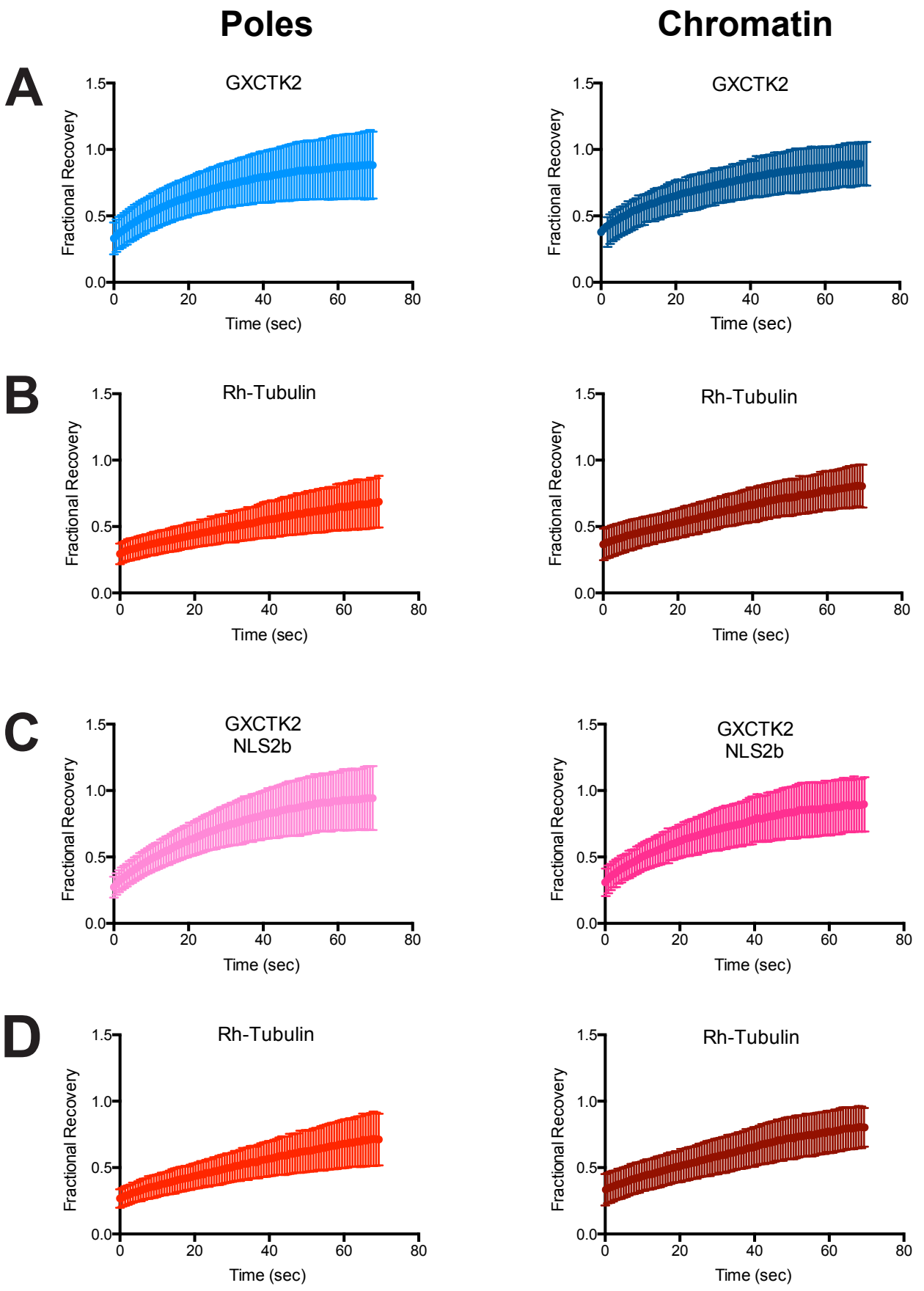

Supplemental Figure Legends

Supplemental Figure 1. Mutation of the NLS in XCTK2 Blocks Binding to Importin β

(A) Quantification of MT bundling in the extracts. Data represent the mean ± SD for 72 fields of view from two independent extracts. (B) Coomassie-stained gel (top) and Western blot (bottom) probed with importin β antibodies (bottom) of GFP immunoprecipitations from *Xenopus* egg extracts in the presence of GFP-XCTK2 (lanes 1-5) or GFP-XCTK2 NLS2b (lanes 6-10) under the indicated conditions. Note that all samples from Figures S1B and S2A were run on a single gel and cut to show the representative lanes in each figure. (C) GFP-XCTK2 or GFP-XCTK2 NLS2b were added to CSF extracts at a five-fold molar excess relative to endogenous XCTK2 in the absence or presence of 10 μM RanQ69L and 30 μM RanT24N (RanQ/T) at 15 minutes post CSF addition. Representative images are shown to illustrate spindle structure and localization. The GFP signal was either scaled equivalently between images (middle) or scaled to enhance the signal to see localization (right). Scale bar, 20 μm. Relates to Figure 1.

Supplemental Figure 2. XCTK2 (122-643) localizes to spindle MTs and does not bind to importin β.

GFP, GFP-XCTK2, GFP-XCTK2 NLS2b, or GFP-XCTK2 (122-643) were added to CSF extracts at a five-fold molar excess relative to endogenous XCTK2 and incubated for 30 min to allow for spindle assembly. (A) Coomassie-stained gel (top) and Western blot with importin β antibodies (bottom) of GFP immunoprecipitations from *Xenopus* egg extracts in the indicated conditions. (B) Representative images are shown to illustrate spindle structure and localization. The GFP signal was either scaled equivalently between images (middle) or scaled to enhance the signal to see localization (right). Scale bar, 20 μm. (C) Western blots of the samples from each reaction to show equal amounts of protein were added to the extract. Relates to Figure 2.

Supplemental Figure 3. Recovery of GFP-XCTK2 and XCTK2 NLS2b is faster than tubulin.

FRAP recovery curves of data from Figure 4. The normalized corrected fluorescence recovery data is plotted as the mean ± SD for the indicated conditions. (A-B) GFP-XCTK2 fluorescence recovery at the poles (left) or the chromatin (right), looking at either the GFP recovery (top) or the rhodamine tubulin recovery (bottom). N = 36 movies. (C-D) GFP-XCTK2 NLS2b fluorescence recovery at the poles (left) or the chromatin (right), looking at either GFP recovery (top) or the rhodamine tubulin recovery (bottom). N = 33 movies. Relates to Figure 4.

Protein	Motor speckle velocity (μm/min)	Number of Speckles	Motor Velocity at Poles (μm/min)	Slowdown (%)	Tubulin Speckle velocity (μm/min)	Number of speckles	Tubulin Velocity at Poles (μm/min)	Slowdown (%)
GXCTK2	5.87 ± 0.18	16,423	4.48 ± 0.34	23.65	2.97 ± 0.15	17,381	2.49 ± 0.2	16.08
GXCTK2 NLS2b	6.05 ± 0.16	16,928	4.81 ± 0.32	20.64	3.15 ± 0.37	29,047	2.79 ± 0.52	11.79
GXCTK2 (122-643)	3.95 ± 0.12	4,692	3.70 ± 0.2	6.49	3.08 ± 0.18	21,532	2.61 ± 0.37	15.40

Supplementary Table I. Values for Fluorescence Speckle Microscopy Analysis of Motor Movement on the Spindle. Relates to Figure 3.

MATERIALS AND METHODS

Constructs and Protein Purification

The GFP-XCTK2 and GFP-XCTK2 NLS2b constructs were described previously [S1]. GFP-XCTK2 (122-643) was created using the pENTR-D/TOPO® Cloning Kit (Invitrogen) by PCR amplification of the coding region corresponding to amino acids 122-643. The pENTR XCTK2 (122-643) entry clone was recombined into the pFBGFP-DEST destination vector. pFBGFP-DEST was created by subcloning the open reading frame of EGFP into pcDNA-DEST53 to replace the cycle 3 GFP coding sequence. All clones were verified by sequencing.

For protein expression of each pFBGFP construct, baculovirus was produced using the Bac-to-Bac baculovirus system (Invitrogen). GFP tagged proteins were then expressed in Sf-9 or High Five insect cells and purified by conventional chromatography as previously described [S2]. Proteins were stored in FPLC buffer (20 mM PIPES pH 6.8, 1 m $MgCl_2$, 1 mM EGTA, 0.1 mM EDTA, 1 mM DTT, 50 µM Mg-ATP, 300 mM KCl, 0.1 µg/ml LPC) with the addition of 10% sucrose, flash frozen in liquid nitrogen and stored at -80^{o}C until used.

Bacterially purified recombinant proteins GST-RanQ69L and GST-RanT24N were induced in BL21(DE3) bacteria. Induction was carried out in the presence of 0.1 mM isopropyl β-D-thiogalactoside (IPTG) for 24 h at 16^{o}C. Each GST-fusion protein was purified with glutathione agarose (Amersham Biosciences) as previously described [S1], dialyzed into dialysis buffer (10 mM HEPES pH 7.7, 100 mM KCl, 25 mM NaCl, 50 mM sucrose, 0.1 mM EDTA, 0.1 mM EGTA), aliquoted, flash-frozen in liquid nitrogen, and stored at -80^{o}C until use.

Protein concentrations were quantified from colloidal Coomassie Blue G-250 stained SDS-polyacrylamide gels using bovine serum albumin (BSA) as a standard. Densitometry was done with ImageJ software (National Institutes of Health).

Western Blot Analysis

For SDS-PAGE, 5 µl of each extract reaction was diluted in 45 µl 2X sample buffer (0.125 M Tris pH 6.8, 4% SDS, 20% glycerol, 4% β-mercaptoethanol, and a trace amount of bromophenol blue) and 15 µl (1.5 µl extract equivalent) was

loaded on a 10% SDS-polyacrylamide gel and transferred to BioTrace NT nitrocellulose (Pall). Blots were then probed with anti-GFP (5 μg/ml) or DM1α (1:1000, Sigma-Aldrich) followed by donkey anti-rabbit IgG HRP-linked whole antibody (1:5000; Amersham) or sheep anti-mouse IgG HRP-linked whole antibody (1:5000; Amersham) and detected with SuperSignal West Pico Chemiluminescent Substrate (Thermo Scientific) according to the manufacturer's directions.

Immunoprecipitations

Immunoprecipitations from *Xenopus* extracts were performed as described previously [S1]. Anti-GFP or non-immune rabbit IgG were covalently linked to the Affi-prep protein A beads (Bio-Rad; Harlow and Lane, 1999). Where indicated, 100 nM purified GFP-XCTK2, GFP-XCTK2 NLS2b, GFP-XCTK2 (122-643) was added to the immunoprecipitation reactions. Equivalent volumes of the eluted protein were electrophoresed on 10% SDS-PAGE and stained with colloidal Coomassie Blue G-250 or transferred to BioTrace NT. Western blots were probed as described above with anti-importin β (1 μg/ml; Sigma-Aldrich) followed by sheep anti-mouse IgG HRP-linked whole antibody (1:5000; Amersham).

Extract Preparation and Spindle Assembly

CSF extract was made from *Xenopus laevis* eggs as previously described [S3]. For fixed spindle assembly assays, CSF extracts were supplemented with X-Rhodamine-labeled tubulin (0.5 μM), 300 sperm nuclei/μl, and the indicated recombinant proteins (GFP, GFP-XCTK2, GFP-XCTK2 NLS2b, GFP-XCTK2 (122-643)) at a final concentration of 50 or 100 nM as indicated in the text (2.5-fold or 5-fold molar excess over the endogenous XCTK2). All fusion proteins were diluted to a 15-fold concentrated stock in CSF-XB buffer, and then equivalent volumes were added to each spindle assembly reaction. RanQ/T extracts were prepared as previously described [S4]. Briefly, CSF extracts were cycled into interphase by the addition of 0.4 mM $CaCl_2$ from a 25X calcium solution (10 mM Hepes, 1 mM $MgCl_2$, 100 mM KCl, 150 mM Sucrose, 10 μg/ml Cytochalasin D, 10 mM $CaCl_2$) for 2 hr at RT. Extracts were placed back on ice for 10 min to allow for MT disassembly. The extract was cycled back into mitosis with fresh CSF extract as described [S5, S6]. Reactions were brought to RT for 15 min to allow for nuclear envelope breakdown after which 10 μM RanQ69L, 30 μM RanT24N, and 100 nM final of the indicated GFP-fusion protein were simultaneously added to the extract. Thirty or 60 min post initiation of spindle assembly, 20 μl of each extract sample was diluted in 1 ml BRB80 (80 mM PIPES, pH 6.8, 1 mM $MgCl_2$, and 1 mM EGTA) containing 30% glycerol (vol/vol) and fixed by the addition of 1 ml of 30% glycerol,

BRB80, and 4% formaldehyde for 10 min at RT. Fixed samples were layered on a 4-ml cushion of BRB80 containing 40% glycerol (vol/vol) and were centrifuged onto coverslips in a Beckman (Fullerton, CA) JS7.5 rotor at 6000 x g for 20 min. Coverslips were postfixed in -20°C methanol for 3 min and rehydrated in TBS-TX (10 mM Tris, pH 7.6, 150 mM NaCl, and 0.1% Triton-X-100). DNA was stained by incubation in 2 µg/ml Hoechst 33342 (Sigma-Aldrich) diluted in TBS-TX, mounted in anti-fade (90% glycerol, 20 mM Tris-HCl, pH 8.8, and 0.5% *p*-phenylenediamine), and sealed with nail polish.

For fluorescent speckle microscopy (FSM) assays, demembranated sperm nuclei at a concentration of 300 sperm/µl were added to extracts and cycled into interphase for 90 min at RT. Extracts were placed back on ice for 10 min to allow for MT disassembly and the extract was cycled back into mitosis with fresh CSF extract. At the time of CSF add-back, GFP-XCTK2 or GFP-XCTK2 NLS2b were added at a final concentration of 6 nM or GFP-XCTK2 (122-643) was added at a final concentration of 20 nM. Rhodamine-labeled tubulin was added at a final concentration of 30 nM and DAPI was added at a final concentration of 1 µg/ml. For imaging, 4 µl of each reaction were squashed under a 22 x 22 mm coverslip and sealed with VALAP (equal volumes of Vaseline, lanolin, and paraffin).

For FRAP assays, demembranated sperm nuclei at a concentration of 300 sperm/µl were added to extracts supplemented with X-Rhodamine-labeled tubulin (0.5 µM) and cycled into interphase for 90 min at RT. At the time of CSF add-back, GFP-XCTK2 or GFP-XCTK2 NLS2b were added at a final concentration of 100 nM and 50 nM respectively. DAPI was added at a final concentration of 1 µg/ml. The extracts were placed at RT for 1 hr for spindle assembly. Samples were processed for live imaging as described above.

Fixed Imaging and Statistical Analysis

Fixed images were acquired on a Nikon Eclipse 90i using a 40X (NA 1.0) Plan Apo, 60X (NA 1.45) Plan Apo VC, or a 100X (NA 1.4) Plan Apo VC objective and a CoolSnap HQ CCD camera (Photometrics). The camera and filters were controlled by Metamorph (Molecular Devices). Images were processed in Adobe Photoshop CS6 and assembled in Adobe Illustrator CS6. For quantification of MT bundling, we used an automated microscope to record a 6 X 6 montage of ~420 X 320 µm individual fields of view from each coverslip. We then scored the number of MT bundles in each field of view

for each of the different conditions. For all data, the mean and the standard deviation (SD), or the standard error of the mean (SEM) were calculated in Excel and plotted in Prism (GraphPad). Statistical significance was determined using a two-tailed Student's *t*-test after taking into account equality of variance between experiments as determined by an F-test. Results were considered statistically significant if $p < 0.05$.

Fluorescent Speckle Microscopy Imaging and Analysis

FSM of *Xenopus* spindles was performed on a Nikon TE2000U inverted microscope equipped with a 60x 1.4NA objective and a Yokogawa CSU-10 spinning disk confocal head (PerkinElmer Life and Analytical Sciences) with laser-based excitation (488 nm and 568 nm) controlled by Nikon Elements. Images were collected on a Cascade-II EMCCD camera (Photometrics). GFP-XCTK2 and GFP-XCTK2-NLS2b were added at a final concentration of 6 nM, and GFP-XCTK2 (122-643) was added at 20 nM final concentration. Sequential images in each channel (green and red) were acquired every 2 sec for a total of 2.5 min. Computer-based image analysis was performed as previously described [S7-S9]. Eight movies were collected and analyzed per condition. For reported velocities/zone, the mean particle velocity was calculated for each movie, and then the average velocity ± standard deviation (SD) was calculated for all movies at each of the indicated zones.

Live FRAP Imaging and Analysis

FRAP of *Xenopus* spindles was performed on a Leica SP5 laser scanning confocal microscope equipped with a 63X (1.2 NA) HCX Plan Apo CS water objective (Leica). LAS software (Leica) was used for confocal imaging in which GFP and rhodamine were excited with the 488 nm and 561 nm laser lines respectively. Photobleaching at each wavelength was performed at 100% laser power, and pre- and post-bleach measurements were recorded at 30% laser power. For each movie, 3 pre-bleach frames were acquired prior to bleaching followed by 100 post-bleach frames at a rate of 0.678 frames/sec. Fluorescence recovery was measured using a custom MATLAB (MathWorks) graphical user interface implementing methods described previously for a similar analysis [S10, S11]. In brief, spindle movies are first aligned to the initial frame using routines incorporating MATLAB 2D affine registration. Regions are then drawn identifying bleached and unbleached reagions of the spindle together with a region having no fluorescent signal. The mean values for each region are taken where the non-fluorescent region is subtracted from the other regions as an offset. To correct for the photobleaching that occurs over the time-course, the background corrected non-bleached regions are fit with linear,

binomial, and exponential functions, and the best fit curve (sum of squared residuals) is used to correct the FRAP recovery data by division. An analytical fitting method is used to find a single exponential function to fit the corrected FRAP recovery curve. The percent recovery was calculated from the asymptotic value of the exponential fit that was normalized to the corrected pre-bleached value for each sample. The $t_{1/2}$ values are reported as the log(2) of the exponential fit. At least 30 spindles were analyzed for each condition.

References

S1. Ems-McClung, S.C., Zheng, Y., and Walczak, C.E. (2004). Importin α/β and Ran-GTP Regulate XCTK2 Microtubule Binding through a Bipartite Nuclear Localization Signal. Mol Biol Cell *15*, 46-57.

S2. Walczak, C.E., Verma, S., and Mitchison, T.J. (1997). XCTK2: A Kinesin-related protein that promotes mitotic spindle assembly in Xenopus laevis egg extracts. J Cell Biol *136*, 859-870.

S3. Murray, A.W. (1991). Cell cycle extracts. Methods Cell Biol *36*, 581-605.

S4. Maresca, T.J., Groen, A.C., Gatlin, J.C., Ohi, R., Mitchison, T.J., and Salmon, E.D. (2009). Spindle assembly in the absence of a RanGTP gradient requires localized CPC activity. Curr Biol *19*, 1210-1215.

S5. Sawin, K.E., and Mitchison, T.J. (1991). Mitotic spindle assembly by two different pathways in vitro. J Cell Biol *112*, 925-940.

S6. Shamu, C.E., and Murray, A.W. (1992). Sister chromatid separation in frog egg extracts requires DNA topoisomerase II activity during anaphase. J Cell Biol *117*, 921-934.

S7. Yang, G., Cameron, L.A., Maddox, P.S., Salmon, E.D., and Danuser, G. (2008). Regional variation of microtubule flux reveals microtubule organization in the metaphase meiotic spindle. J Cell Biol *182*, 631-639.

S8. Yang, G., Houghtaling, B.R., Gaetz, J., Liu, J.Z., Danuser, G., and Kapoor, T.M. (2007). Architectural dynamics of the meiotic spindle revealed by single-fluorophore imaging. Nat Cell Biol *9*, 1233-1242.

S9. Houghtaling, B.R., Yang, G., Matov, A., Danuser, G., and Kapoor, T.M. (2009). Op18 reveals the contribution of nonkinetochore microtubules to the dynamic organization of the vertebrate meiotic spindle. Proc Natl Acad Sci U S A *106*, 15338-15343.

S10. Rizk, R.S., Bohannon, K., Wetzel, L., Powers, J.A., Shaw, S.L., and Walczak, C.E. (2009). MCAK and paclitaxel have differential effects on spindle organization and microtubule dynamics. Mol Biol Cell *20*. 1639-1651.

S11. Walczak, C.E., Rizk, R.S., and Shaw, S.L. (2010). The use of fluorescence redistribution after photobleaching for analysis of cellular microtubule dynamics. Methods Cell Biol *97*, 35-52.